AJNR

Clinical Application of Readout-Segmented–Echo-Planar Imaging for Diffusion-Weighted Imaging in Pediatric Brain

S.J. Holdsworth, K. Yeom, S. Skare, A.J. Gentles, P.D. Barnes and R. Bammer

AJNR Am J Neuroradiol 2011, 32 (7) 1274-1279
doi: https://doi.org/10.3174/ajnr.A2481
http://www.ajnr.org/content/32/7/1274

ORIGINAL RESEARCH

Clinical Application of Readout-Segmented–Echo-Planar Imaging for Diffusion-Weighted Imaging in Pediatric Brain

S.J. Holdsworth
K. Yeom
S. Skare
A.J. Gentles
P.D. Barnes
R. Bammer

BACKGROUND AND PURPOSE: RS-EPI has been suggested as an alternative approach to EPI for high-resolution DWI with reduced distortions. To determine whether RS-EPI is a useful approach for routine clinical use, we implemented GRAPPA-accelerated RS-EPI DWI at our pediatric hospital and graded the images alongside standard accelerated (ASSET) EPI DWI used routinely for clinical studies.

MATERIALS AND METHODS: GRAPPA-accelerated RS-EPI DWIs and ASSET EPI DWIs were acquired on 35 pediatric patients using a 3T system in 35 pediatric patients. The images were graded alongside each other by using a 7-point Likert scale as follows: 1, nondiagnostic; 2, poor; 3, acceptable; 4, standard; 5, above average; 6, good; and 7, outstanding.

RESULTS: The following were the average scores for EPI and RS-EPI, respectively: resolution, 3.5/5.2; distortion level, 2.9/6.0; SNR, 3.4/4.1; lesion conspicuity, 3.3/5.9; and diagnostic confidence, 3.2/6.0. Overall, the RS-EPI had significantly improved diagnostic confidence and more reliably defined the extent and structure of several lesions. Although ASSET EPI scans had better SNR per scanning time, the higher spatial resolution as well as reduced blurring and distortions on RS-EPI scans helped to better reveal important anatomic details at the cortical-subcortical levels, brain stem, temporal and inferior frontal lobes, skull base, sinonasal cavity, cranial nerves, and orbits.

CONCLUSIONS: This work shows the importance of both resolution and decreased distortions in the clinics, which can be accomplished by a combination of parallel imaging and alternative *k*-space trajectories such as RS-EPI.

ABBREVIATIONS: ASSET = array spatial sensitivity encoding technique; DTI = diffusion tensor imaging; DWI = diffusion-weighted imaging; EPI = echo-planar imaging; FSE = fast spin-echo; GRAPPA = generalized autocalibrating partially parallel acquisition; PROPELLER = periodically rotated overlapping parallel lines with enhanced reconstruction; RS-EPI = readout-segmented–echo-planar imaging; SNR = signal intensity–to-noise ratio; TE_{min} = minimum TE

In the past decade, DWI has emerged as an important technique not only in stroke imaging but also in various other clinical settings. DWI often enables detection of subtle lesions, narrows the differential diagnoses, and provides insight into the disease time course. When combined with conventional MR imaging, DWI has become a powerful tool in characterizing tissue physiology. DWI particularly plays an important role in pediatric neuroradiology, in which there are multiple pathologic processes sensitive to diffusion abnormality, including primary or secondary energy failure, toxic-metabolic disorders, seizure, trauma (accidental or nonaccidental), demyelination, tumors, infection, and others.

Single-shot EPI is currently the sequence used most routinely for clinical studies in DWI. However, EPI has geometric distortion and signal-intensity drop-out (particularly at tissue-air boundaries) and overall T2*-induced blurring. With increasing field strength, these effects are even more pronounced. The introduction of parallel imaging has helped to reduce these artifacts and to significantly improve the quality of EPI DWI. However, EPI in combination with parallel imaging can reduce distortion only to a certain point. Because distortion is proportional to the matrix size in EPI, distortion and blurring artifacts can become increasingly prohibitive at higher resolutions.

There are other methods that can reduce distortion, one being interleaved (or multishot) EPI; however, this has ghosting artifacts in the presence of motion. Despite the absence of geometric-distortion artifacts, FSE-based sequences have also been difficult to use in clinical practice, mainly because they have a long scanning time and violate the Carr-Purcell-Meiboom-Gill condition. Another way to reduce distortion is by using RS-EPI.[1-4] Figure 1 compares the EPI and the RS-EPI pulse-timing diagram and *k*-space trajectory. By acquiring several adjacent segments or "blinds" in RS-EPI (in this case 7 blinds), one can reduce geometric distortion by a factor proportional to the blind width (limited by the slew-rate constraint). Because of the much higher bandwidth per pixel, RS-EPI is capable of acquiring images with significantly reduced distortion compared with EPI and offers the potential of getting DWIs comparable with regular anatomic scans.[4] Note that for RS-EPI, one needs to correct for the effects of minuscule motion that occurs between blinds; this process is known

Received June 18, 2010; accepted after revision December 3.

From the Department of Radiology, Stanford University, Stanford, California.

This work was supported by grants from the National Institutes of Health (1R01 EB008706, 1R01 EB008706S1, 5R01 EB002711, 1R01 EB006526, 1R21 EB006860); the Center of Advanced MR Technology at Stanford (P41RR09784); and the Lucas Foundation, Oak Foundation, and the Swedish Research Council (K2007–53P-20322–01-4).

Please address correspondence to Roland Bammer, PhD, Stanford University, Department of Radiology, Lucas Center, 1201 Welch Rd, Stanford, CA 94305-5488; e-mail: rbammer@stanford.edu

DOI 10.3174/ajnr.A2481

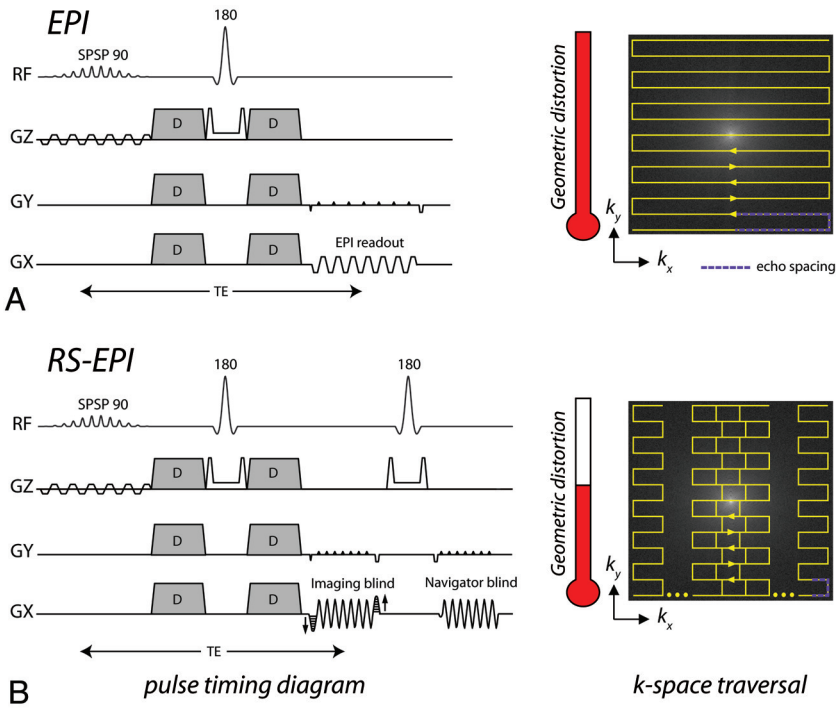

Fig 1. Pulse-timing diagram and *k*-space traversal of the (*A*) EPI and (*B*) RS-EPI trajectories. In RS-EPI, each imaging blind is accompanied by a navigator blind acquired at the center of *k*-space (not shown in the *k*-space traversal schematic) to perform a phase correction that will correct for phase differences between blinds. The purple dotted line denotes the "echo-spacing"—that is, the time between consecutive echoes in an EPI echo-train. The amount of geometric distortion in an image is proportional to this. The distortion meter shows the resulting distortion reduction (drawn to scale) with the use of RS-EPI, assuming a blind width of 64 and a matrix size of 192 × 192.

as "phase correction." To do this, an extra navigator blind is acquired, and each individual blind can be phase-corrected. The navigator blind can also be used to correct for motion between blinds in the presence of rigid-body motion. Thus, RS-EPI can be made robust toward motion,[4] while keeping distortion minimized and the scanning time reasonable for routine clinical use.

The purpose of this study was to implement GRAPPA-accelerated RS-EPI DWI on a clinical scanner at 3T for pediatric imaging and to demonstrate patient data. To demonstrate the relative importance of higher resolution and reduced distortion, we performed a comparative evaluation between our optimized sequence with a tailored reconstruction and what is currently state-of-the-art for DWI. Specifically, we acquired RS-EPI diffusion data on 35 pediatric patients and compared the image quality with images acquired with the standard accelerated (ASSET) EPI DWI used routinely for clinical studies at our pediatric hospital. The images were evaluated by a neuroradiologist (K.Y.) on the basis of 5 measures of image quality.

Materials and Methods

Clinical Patients

Thirty-five consecutive pediatric patients who were undergoing brain MR imaging at our institution were prospectively enrolled in this study and evaluated. Nineteen patients were female and 15 were males between the ages of 1 day to 18 years of age and were imaged for a variety of clinical indications. All scans were obtained under approval of the review board from our institution, and written informed consent was obtained from subjects' parents.

MR Imaging

RS-EPI and single-shot EPI images were acquired on 35 patients by using a 3T whole-body DVMR 750 system (GE Healthcare, Milwaukee, Wisconsin) with an 8-channel head coil and a high-performance gradient system (gradient strength = 50 mT/m, slew rate = 200 mT/m/s). The following parameters were used for both sequences: FOV = 20 cm, section thickness = 4 mm, TR = 3 seconds, 1 b = 0 and 3 diffusion directions with b = 1000 s/mm^2 (xyz diffusion encoding). The routine ASSET-accelerated EPI sequence used a matrix size of 128 × 128, an acceleration factor R = 2, TE_{min} of 80 ms, partial Fourier encoding with 16 overscans, and a scanning time of 50 seconds. RS-EPI used a twice-refocused diffusion preparation with a matrix size of 192 × 192, 7 blinds (width = 64, blind overlap factor = 57%), R = 3, NEX of 3, TE_{min} = 69 ms, partial Fourier encoding with 18 overscans, and a scanning time of 4:12 minutes.

Note that the ASSET-accelerated EPI sequence used here is the current standard clinical protocol used at our institution. The matrix resolution of 128 × 128 has been established in our practice to keep the distortion level and T2 shinethrough within reasonable limits, while the acceleration factor has been kept at 2 (for use with our 8-channel coil) to avoid aliasing artifacts common with the sensitivity encoding–based reconstruction provided by our vendor. Similarly, the RS-EPI sequence parameters used in this study have been established by the authors as an acceptable trade-off between distortion reduction and SNR.

A detailed description of the postprocessing for RS-EPI is found elsewhere.[4] An important part of the reconstruction to note here, however, is that each blind was phase-corrected (with the use of the navigator blind) by using a triangular windowing approach,[5] which allowed complex signal-intensity averaging instead of magnitude averaging that is usually used for DWI. Here, a window radius of 0.25

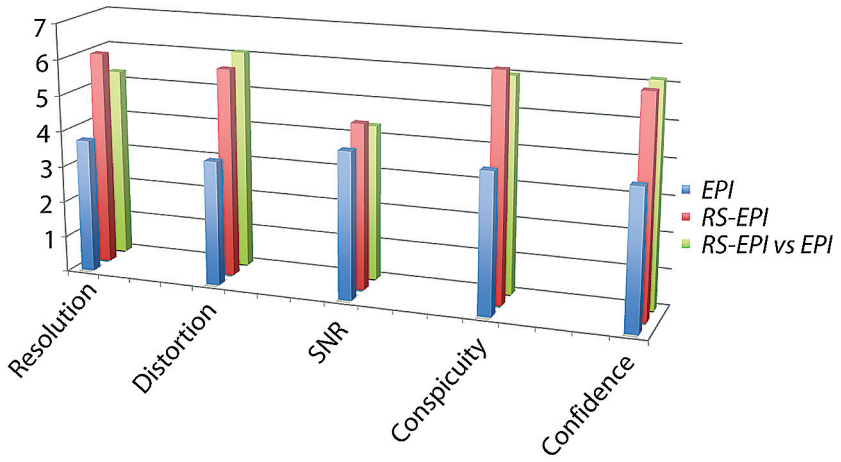

Fig 2. Comparison between the routine ASSET-accelerated EPI sequence and our implementation of RS-EPI in terms of 5 categories averaged over 35 patients.

was chosen, because a previous clinical study[6] demonstrated that under most circumstances this "minimal" phase-correction is sufficient to correct for phase artifacts seen in EPI due to brain pulsation.

Image Assessment

A pediatric neuroradiologist (blinded to which sequence was reviewed) evaluated the iso-DWIs acquired on the 35 patients by using RS-EPI and EPI, scoring them in terms of resolution, distortion level, SNR, lesion conspicuity, and diagnostic confidence on a 7-point Likert scale as follows: 1, nondiagnostic; 2, poor; 3, acceptable; 4, standard; 5, above average; 6, good; and 7, outstanding. Note that the SNR was not normalized for scanning time. First, the images were scored independently for each sequence, followed by a re-evaluation of the RS-EPI images with the EPI and RS-EPI datasets viewed together. Finally, a direct side-by-side comparison of the images was performed (RS-EPI alongside EPI) on all evaluation criteria, and an overall sequence preference was thereby selected on a "winner-takes-all" basis. While the independently viewed images gave more room for subjective variance, the direct comparison allowed all 5 measures of image quality to weigh into the radiologist's decision. Wilcoxon signed rank tests were used to assess the radiologist's ratings. Final diagnosis was made by another pediatric neuroradiologist (P.D.B.) by using all clinical and imaging material (including previous examinations if available) and served as ground truth for the study.

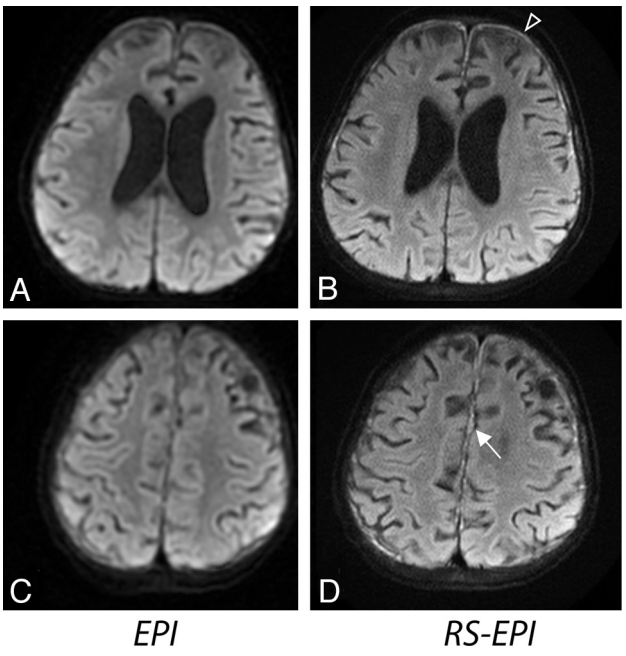

Fig 3. An 18-month-old boy presenting with subdural empyema. *A* and *B*, Abscess depicted with greater diagnostic confidence on RS-EPI. *C* and *D*, Pus present along the falx on RS-EPI (*D*), not well seen on EPI (*C*).

Results

The average scores calculated across 35 patients are shown in Fig 2. The following scores were given to EPI, RS-EPI, and RS-EPI re-evaluated alongside the EPI, respectively: resolution, 3.5/5.8/5.2; distortion level, 2.9/5.5/6.0; SNR, 3.4/4.2/4.1; lesion conspicuity, 3.3/6.0/5.9; and diagnostic confidence, 3.2/5.8/6.0. The *P* values for EPI versus RS-EPI viewed first independently and then as a direct comparison, were as follows: resolution, 1.9×10^{-6} / 1.2×10^{-6}; distortion level, 1.3×10^{-6} / 9.5×10^{-7}; SNR, .006/.007; lesion conspicuity, .005/.007; and diagnostic confidence, 1.3×10^{-6} / 1.9×10^{-6}. Overall, the RS-EPI had significantly improved diagnostic confidence. RS-EPI identified a lesion not found by EPI in 1 patient (a small subdural empyema, Fig 3) and more accurately defined the extent and location of the lesions, such as ischemic injury, metabolic disorder (Fig 4), a cystic encephalomalacia (Fig 5), and a skull base tumor. In 1 case, RS-EPI (Fig 6*B*) correctly identified a false-positive ischemic lesion in the temporal lobe seen on EPI in a patient with Moyamoya disease (Fig 6*A*). In another case, RS-EPI (Fig 6*D*) correctly identified a false-negative ischemic lesion in the temporal lobe in a postoperative patient with Moyamoya disease, where this was presumed to be a post-operative blood-product artifact on EPI. (Fig 6*C*).

RS-EPI also reduced distortion in areas adjacent to tissue-air or bone interfaces from signal-intensity pile-up effects (Fig 6*A, -B*) and gave increased diagnostic confidence in areas adjacent to the auditory canal in a patient with tumor (Fig 7). In several patients, EPI had elevated gray/white matter contrast on iso-DWI due to a more pronounced T2 shinethrough effect from the longer TE of EPI as shown in Fig 8 (note that this did not occur for RS-EPI even though RS-EPI used twice-refocused diffusion preparation which prolongs TE). These equiv-

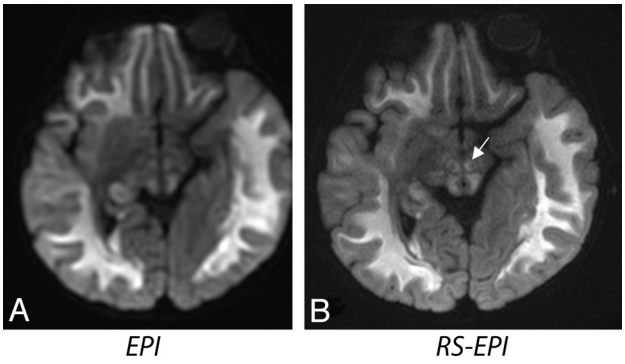

Fig 4. A 10-month-old girl with Leigh disease. RS-EPI shows exquisite resolution at the level of the brain stem, specifically in the midbrain. The red nucleus is also better defined on RS-EPI (*white arrow*).

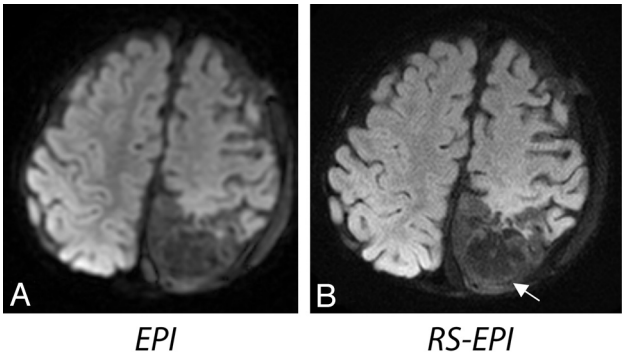

Fig 5. A 10-month-old boy presenting with cystic encephalomalacia. RS-EPI demonstrates cystic encephalomalacic changes with higher resolution.

ocal signal-intensity high intensities occasionally led to a decreased diagnostic confidence level.

In 12 patients, the EPI scans had mild-to-severe "wormlike" artifacts that often corrupted several sections, generally in a supratentorial location, though these were not accounted for when considering the final sequence preference because they can be attributed to a reconstruction flaw of the product sequence related to partial Fourier reconstruction.[7] The RS-EPI dataset was preferred overall in all except 2 patients due to the presence of destructive phase-cancellation artifacts on RS-EPI arising from pulsatile brain motion. By using the full triangular-window radius, we found that these artifacts could be removed in both datasets—with little effect on the noise characteristics in the final iso-DWI.

Although ASSET EPI scans had better SNR efficiency (ie, SNR per square root of the scanning time), the higher spatial resolution as well as reduced blurring and distortions on RS-EPI scans improved anatomic details at the cortical-subcortical levels, brain stem, temporal and inferior frontal lobes, skull base, nasoethmoid region in interior cranial fosa, the cranial nerves, and the orbits. Exquisite orbital detail was delineated in all 35 RS-EPI scans. Figure 9 shows side-by-side comparisons between ASSET EPI (top) and RS-EPI (bottom) DWIs in 2 patients and highlights these findings. Figure 9*A* shows a patient with a small subdural empyema in the middle cranial fossa, which was equivocal on conventional ASSET EPI, mostly because of poor resolution and profound signal intensity loss along the orbits. On RS-EPI, orbital details such as the optic nerve and medial rectus muscle were more clearly outlined compared with ASSET EPI. Also, due to less distortion, RS-EPI enabled tumor delineation more clearly, even at the anterior skull base and near air–soft tissue interfaces, such as the nasoethmoid. This illustrates a potential clinical use of RS-EPI in evaluating highly cellular pediatric tumors, such as neuroblastoma, retinoblastoma, and rhabdomyosarcoma, which have a propensity to occur in regions susceptible to distortion.

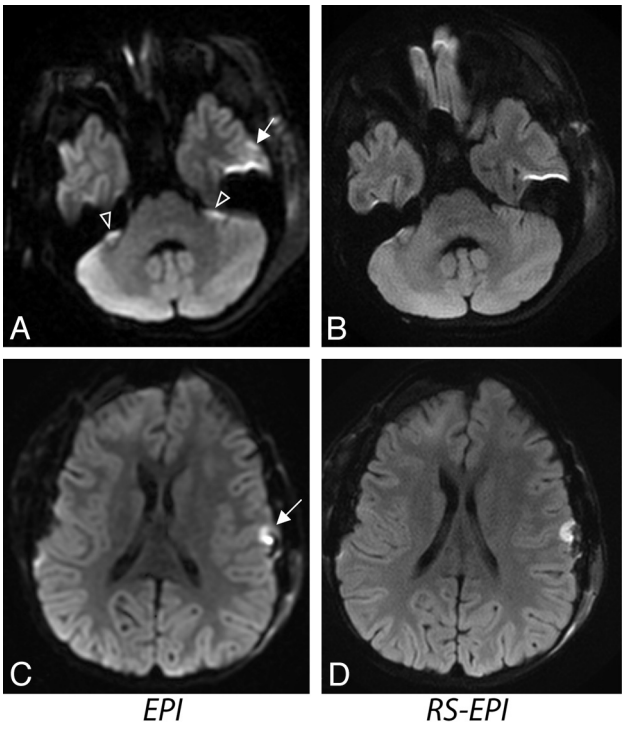

Fig 6. Two patients with Moyamoya disease. *A* and *B*, An 8-year-old girl presenting with possible infarct or blood product at the surgical site on EPI (*solid white arrow*). The absence of these distortion artifacts on RS-EPI makes this confidently negative. The open white arrows indicate undesirable brightening of the flocculus due to susceptibility artifacts from the brain/bone interface. *C* and *D*, A 3-year-old boy presenting with possible postoperative blood-product artifacts on EPI (*white arrow*), but the lesion appears more suspicious for an ischemic lesion on RS-EPI. On closer inspection, the lesion demonstrates subtle cortical T2 high intensity on the T2 FSE sequence, confirming the suspicion that this represents a true ischemic focus, rather than distortion related to postoperative changes. These 2 cases demonstrate that RS-EPI is both sensitive and specific.

Discussion

As shown in Fig 2, RS-EPI outperformed the product ASSET EPI sequence in all categories selected for image quality. However, because the SNR was not normalized for scanning time, in practice EPI would outperform RS-EPI for SNR because it covers *k*-space more efficiently. Figures 3–9 show cases in which RS-EPI had increased diagnostic confidence and/or improved lesion conspicuity. The increased clarity and ability to resolve small neuroanatomic structures with RS-EPI was particularly noticeable in areas of high susceptibility such as inferior frontal lobes, temporal lobes, and posterior fossa.

In addition, RS-EPI did not have the detrimental wormlike artifacts as seen in 12 patients on EPI. These wormlike artifacts arise from brain motion occurring during the diffusion-encoding gradients. A possible explanation for their presence on EPI (and not on RS-EPI) is due to the application of the phase-

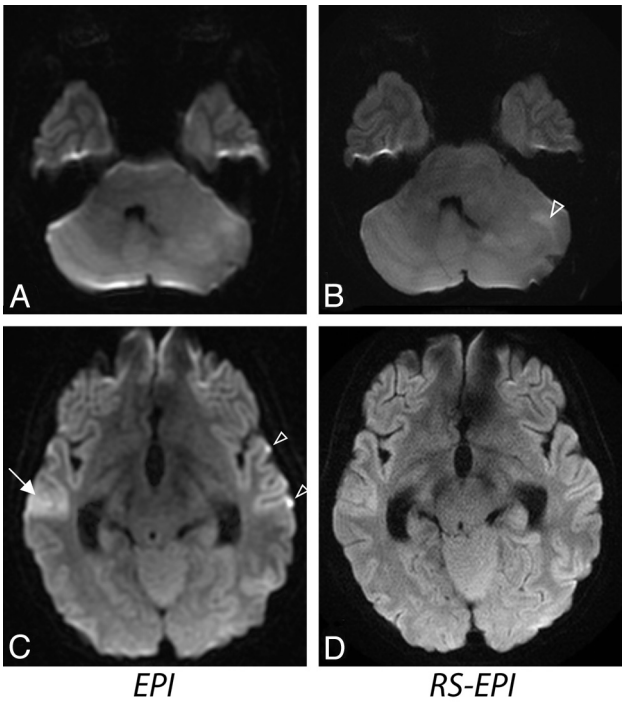

Fig 7. Two sections from a patient with diffuse infiltrating anaplastic astrocytoma (a 14-year-old girl). *A* and *B*, DWI shows areas of increased cellularity (*open white arrow*). *C* and *D*, Areas of increased signal intensity on EPI (*white arrow*) suggest the possibility of cortical and subcortical tumor involvement, which may be seen with gliomatosis or diffuse infiltrating glioma. Reduction of distortion in RS-EPI shows a normal cortical ribbon. Also, the open arrows show areas of increased distortion on EPI compared with RS-EPI.

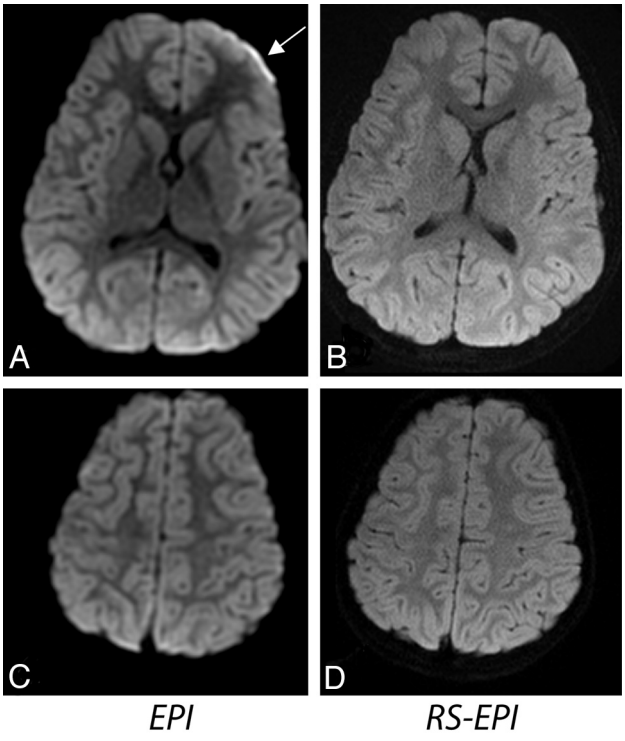

Fig 8. Two sections from an 8-year-old female patient. *A*, Distortion artifacts on EPI could be confused with subdural hemorrhage or empyema. This artifact disappears on RS-EPI (*B*). *A,C,* Elevated contrast on EPI, not appearent on RS-EPI (*B,D*), could be confused with diffuse cortical ischemic injury, encephalitis, or even seizure-related changes.

correction in RS-EPI before partial Fourier reconstruction,[8] while phase correction can ensure the "refocusing" of the signal intensity, thus providing a more reliable phase map for the partial Fourier reconstruction.

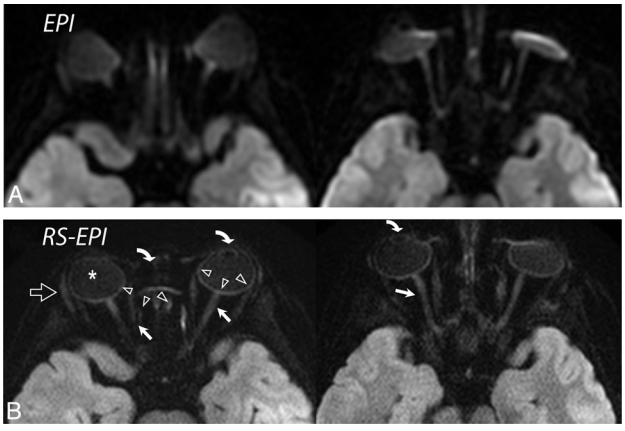

Fig 9. *A*, ASSET-accelerated (×2) diffusion-weighted single-shot EPI in 2 different subjects (a 3-year-old girl and a 10-year-old boy) and their corresponding diffusion-weighted RS-EPI scans. *B*, ASSET EPI scans have a better SNR, but orbital anatomy, such as the lens (*curved arrows*), optic nerve (*arrows*), sclera (*arrowheads*), vitreous humor (*asterisk*), and lacrimal glands (*open arrow*), are clearly better depicted on RS-EPI than on conventional ASSET-accelerated EPI scans.

SNR aside, RS-EPI was chosen as the overall preference for all except 2 patients due to the presence of phase artifacts on DWI. These artifacts were later removed by increasing the triangular window used for phase correction of each individual diffusion-weighted component image to the full *k*-space radius ($r = 1.0$). A consequence of using $r = 1.0$ is that almost the entire phase of each component image is removed, and the final iso-DWI approaches "magnitude averaging"—in other words, moves away from background noise-suppressing complex averaging and increases the hazy-appearing Rician noise floor in the final iso-DWI. However, due to the use of a small number of diffusion directions, the iso-DWIs in this study came with only a modest increase in the noise floor because the noise-cancelling effect of complex averaging is less apparent with the use of a small number of diffusion directions. Thus, for standard RS-EPI DWI, we suggest the use of $r = 1.0$ to help avoid the presence of phase artifacts from pulsatile brain motion.

Despite its obvious diagnostic benefits, reports on the use of DWI to diagnose orbital pathology have been relatively scarce. Studies that have investigated orbital pathology by using standard DWI are limited in lesion detection due to poor resolution and distortion in the orbits.[9,10] Optic neuritis is one of the early hallmarks of multiple sclerosis; other studies have also investigated the use of DWI and DTI as tools for optic nerve evaluation.[11,12] To mitigate distortion, the authors used a reduced FOV technique that leveraged on zonally oblique multisection EPI. Another study that also examined the application of diffusion imaging in the optic nerve pathology used a localized volume 3D single-shot stimulated-echo acquisition mode EPI approach.[13] Future work could be to reduce distortion even further by combining these localized volume-selection approaches with RS-EPI, as has been done for spine imaging.[14]

Other methods used for reducing distortion are FSE methods, such as PROPELLER or split-echo acquisition of FSE signals. These methods could potentially provide high-quality

images as well but can have prohibitively long scanning times for clinically useful resolutions. The pseudo-EPI nature of RS-EPI makes it much faster than FSE methods because more *k*-space is covered in a given TR, and RS-EPI is also less intensive on the specific absorption rate. While PROPELLER-based techniques are well-suited for correcting for motion, previous work has shown that RS-EPI also has robust motion-correction capabilities, even without requiring much overlap of each EPI *k*-space segment.[4]

Here, we demonstrate the clinical feasibility of RS-EPI and compare its diagnostic capability against ASSET EPI routinely used in clinical practice. RS-EPI reduces artifacts that could be mistaken for pathologic brain lesions, while enhancing lesions that could be attributed to susceptibility artifacts. Furthermore, reduced distortion and high-resolution capability of RS-EPI in evaluating orbital and sinonasal pathology further highlight its potential future application in head and neck imaging, including imaging of congenital lesions such as dermoid/epidermoid, infectious process, and various types of cellular tumors.

There are some important differences between the 2 sequences compared in this work: ASSET EPI was the only DWI sequence provided by the vendor, with an acceleration factor of $R = 2$ to avoid aliasing and a matrix size of 128×128 to keep distortion within acceptable limits. With our implementation of GRAPPA RS-EPI, however, GRAPPA can achieve a higher acceleration factor, while RS-EPI can be acquired at a higher resolution because of the reduced distortion. Because we only had the option of performing RS-EPI together with the standard DWI protocol (ASSET EPI), our aim was to show the benefit of our implementation of RS-EPI in the clinical setting. While the benefit of GRAPPA-accelerated RS-EPI over GRAPPA-accelerated EPI has been demonstrated on volunteers,[2] the relative utility of RS-EPI in this context has yet to be proved in the clinical setting. This important investigation is the aim of future work. Also a longer scanning time was necessary for RS-EPI because of the higher acceleration factor as well as the shorter data acquisition per TR, both of which result in a decreased normalized SNR compared with ASSET EPI. The SNR reduction is the greatest disadvantage of RS-EPI; however, this may be well-invested for the diagnostic work-up of lesions occurring in susceptible locations in the brain as well as in the head and neck.

Other limitations of this work are the use of only a single rater for this study and the fact that not all major classes of pathology that could potentially benefit from this technique were represented in this sample (for example, trauma). In addition, due to the increased scanning time, the benefits of this technique may be limited in an acute stroke setting where time is critical.

The work shows that RS-EPI offers a useful alternative to diffusion-weighted single-shot EPI for evaluating regions of the brain susceptible to distortion. RS-EPI was useful for problem-solving lesions that were equivocal on standard DWI and thereby increased the overall diagnostic accuracy. Furthermore, RS-EPI may be used to provide additional pathologic detail in the orbits, skull base, and sinonasal cavity, areas that often remain nondiagnostic and frequently overlooked by standard EPI DWI. Currently, we have used 2 protocols optimized for the given sequence and system hardware under evaluation. Further work is underway to evaluate the individual contributions (ie, reduction factor and resolution) to the improved ratings on RS-EPI. In conclusion, this study shows the importance of improved resolution and distortion in the clinical application of diffusion imaging, which can be accomplished by performing parallel imaging with GRAPPA calibration, combined with alternative *k*-space trajectories such as RS-EPI.

Acknowledgments

We thank Serman Lim, Alfred Barikdar, Allan White, Young Chang, Harold Estrada, Liz Ellison, and Abbie Bird for their assistance with the patient studies.

References

1. Porter D, Mueller E. **Multi-shot diffusion-weighted EPI with readout mosaic segmentation and 2D navigator correction**. In: *Proceedings of the 11th Annual Meeting of the International Society for Magnetic Resonance in Medicine,* Kyoto, Japan, May 15–21, 2004:442
2. Holdsworth SJ, Skare S, Newbould RD, et al. **Readout-segmented EPI for rapid high resolution diffusion imaging at 3T.** *Eur J Radiol* 2008;65:36–46
3. Porter DA, Heidemann RM. **High resolution diffusion-weighted imaging using readout-segmented echo-planar imaging, parallel imaging and a two-dimensional navigator-based reacquisition.** *Magn Reson Med* 2009;62:468–75
4. Holdsworth SJ, Skare S, Newbould RD, et al. **Robust GRAPPA-accelerated diffusion-weighted readout-segmented (RS)-EPI.** *Magn Reson Med* 2009;62:1629–40
5. Pipe JG, Farthing VG, Forbes KP. **Multishot diffusion-weighted FSE using PROPELLER MRI.** *Magn Reson Med* 2002;47:42–52
6. Skare S, Holdsworth SJ, Newbould RD, et al. **On the battle between Rician noise and phase-interferences in DWI**. In: *Proceedings of the 17th Annual Meeting of the International Society for Magnetic Resonance in Medicine,* Honolulu, Hawaii. April 18–24, 2009:1409
7. Storey P, Frigo FJ, Hinks RS, et al. **Partial k-space reconstruction in single-shot diffusion-weighted echo-planar imaging**. *Magn Reson Med* 2007:57:614–19
8. Holdsworth SJ, Skare S, Bammer R. **On the application of phase correction and use of k-space entropy in partial Fourier diffusion-weighted EPI**. In: *Proceedings of the 17th Annual Meeting of the International Society for Magnetic Resonance in Medicine,* Honolulu, Hawaii. April 18–24, 2009:4617
9. Kapur R, Sepahdari AR, Mafee MF. **MR imaging of orbital inflammatory syndrome, orbital cellulitis, and orbital lymphoid lesions: the role of diffusion-weighted imaging.** *AJNR Am J Neuroradiol* 2009;30:64–70
10. Sepahdari AR, Aakalu VK, Kapur R, et al. **MRI of orbital cellulitis and orbital abscess: the role of diffusion-weighted imaging.** *AJR Am J Roentgenol* 2009;193:W244–50
11. Wheeler-Kingshott CA, Parker GJM, Symms MR, et al. **ADC mapping of the human optic nerve: increased resolution, coverage, and reliability with CSF-suppressed ZOOM-EPI.** *Magn Reson Med* 2002;47:24–31
12. Wheeler-Kingshott CA, Trip SA, Symms MR, et al. **In vivo diffusion tensor imaging of the human optic nerve: pilot study in normal controls.** *Magn Reson Med* 2006;56:446–51
13. Jeong E, Kim S, Kholmovski EG, et al. **High-resolution DTI of a localized volume using 3D single-shot diffusion-weighted stimulated echo-planar imaging (3D ss-DWSTEPI).** *Magn Reson Med* 2006;56:1173–81
14. Holdsworth SJ, Skare S, O'Hallaran R, et al. **Reduced-FOV diffusion imaging with ZOnal Oblique Multislice (ZOOM) combined with readout-segmented (RS)-EPI**. In: *Proceedings of the 18th Annual Meeting of the International Society for Magnetic Resonance in Medicine,* Stockholm, Sweden. May 1–7, 2010:1611